

Study of the Effect of Strontium (Sr) on the Nucleation of Eutectic Silicon (Si) in High Purity Hypoeutectic Al-5Si Alloys

Muhammad Zarif*, Brian McKay**, Jiehua Li* and Peter Schumacher*, ***

* Chair of Casting Research, University of Leoben, Austria

** BCAST Brunel University, Uxbridge, Middlesex, U.K.

*** Austrian Foundry Research Institute, Leoben, Austria

Received: September 30, 2010; accepted: October, 13, 2010

Abstract: High purity Al-5Si (wt. %) master alloys containing different levels of Sr additions were manufactured in an arc melter under high vacuum. The alloys were melt-spun which resulted in the production of thin ribbons. The microstructure of the ribbons consisted of Al matrix and entrained eutectic droplets. The ribbons were subsequently investigated using differential scanning calorimetry (DSC) and conventional transmission electron microscopy (CTEM) to examine the effect of Sr on the droplet undercooling and nucleation of eutectic silicon. The results indicate that the addition of Sr increases the eutectic droplet nucleation undercooling (ΔT). This may be due to Sr poisoning of the AIP phase.

Untersuchung des Einflusses von Strontium (Sr) auf die Keimbildung des eutektischen Siliziums (Si) in hochreinen untereutektischen AlSi5-Legierungen

Zusammenfassung: In dieser Arbeit wurden hochreine AlSi5-Vorlegierungen mit unterschiedlichen Gehalten an Sr untersucht. Hergestellt wurden die Legierungen in einem Elektrolichtbogenofen unter Hochvakuum. Die Legierungen wurden mittels Schmelzspinnen zu dünnen Bändern verarbeitet, wobei das Gefüge der hergestellten Bänder aus der Al-Matrix und tröpfchenförmigen eingeschlossenen Anteilen an Eutektikum bestand. Anschließend wurden die Bänder mittels dynamischer Differenzkalorimetrie (DSC) und konventioneller Transmissionselektronenmikroskopie (CTEM) untersucht, um den Einfluss von Sr auf die Unterkühlung und Keimbildung des eutektischen Si zu ermitteln. Die Ergebnisse zeigen, dass die Zugabe von Sr die eutektische Keimbildungsunterkühlung (ΔT) erhöht. Es wird angenommen, dass der Grund hierfür eine Sr-Vergiftung der AIP-Phase ist.

Correspondence author:

Muhammad Zarif

Lehrstuhl für Gießereikunde, Montanuniversität Leoben,
 Franz-Josef-Straße 18, 8700 Leoben, Austria
 e-mail: zafarzarif@yahoo.com,
 muhammad-zafar.zarif@stud.unileoben.ac.at

1. Introduction

Modification^{1, 2} of the Al-Si eutectic in hypoeutectic alloys plays an important role in the enhancement of the mechanical properties. The modification phenomenon was first discovered by Pacz³ in 1920. The improvement in the mechanical properties is believed to be due to the change in the size and morphology of eutectic silicon. It is well established that nucleation and growth during solidification⁴⁻⁶ plays a key role in modification. However, the detailed nucleation mechanism is still not well understood. The nucleation is difficult to study because of the complex role of the inherent impurities present in Al alloys. The novel entrained droplet technique first used by Wang and Smith⁷ has proved useful in isolating extraneous impurities. The technique involved the study of nucleation kinetics in small eutectic liquid droplets and was developed further by Cantor and co-workers⁸⁻¹⁰ to study the different alloy systems using rapid solidification techniques.

Ho et al.⁶ studied the role of traces of phosphorus on nucleation in high purity Al-Si alloys. They proposed that only 0.25–2 ppm phosphorus is sufficient to form AIP. Mondolfo⁴ reported the poisoning effect of sodium on AIP and concluded that the formation of Na₃P might reduce the amount of AIP hence increases the eutectic silicon nucleation and growth temperature i.e. higher undercooling (ΔT). Later, Cantor et al.¹¹ confirmed this finding; they found that the ppm addition of sodium increased the eutectic droplet nucleation undercooling (ΔT). The AIP is believed to be the potent nucleation site for eutectic silicon^{4, 11, 12}.

Other modifiers i.e. Sr, Ca, Sb and Ce are believed to behave in a similar fashion as sodium¹³. A recent publication¹⁴ proposed that the addition of strontium caused the formation of Al₂Si₂Sr intermetallics. These intermetallic compounds may consume the AIP phase, thereby reducing the number of nucleated eutectic grains.

The main objective of this paper is to investigate in detail the effect of different levels of strontium on eutectic silicon nucleation by using an entrained droplet technique in an Al-

5Si (wt. %) alloy. The nucleation events in samples were subsequently analyzed using DSC (Differential Scanning Calorimetry) and CTEM (Conventional Transmission Electron Microscopy). Thermodynamic simulations were then performed to predict the phases formed during solidification.

2. Experimental Methods

A series of Al-Si and Al-Si-Sr master alloys, with controlled additions of strontium were manufactured, using 4N (99.99 wt. %) high purity electrolytically refined Al (Hydro Aluminium High Purity GmbH), and with two different purity levels of silicon 5N (99.999 wt. %) and 4N (99.99 wt. %), (from Siltronic AG and SAG GmbH, respectively). For the additions of Sr, an Al-3.59Sr (wt. %) master alloy was produced, using 4NAI + 99 wt. % Sr (Johnson Matthey Plc). Phosphorous additions were made by Al-19 wt. %Cu-1.4 wt. %P rod, (Technologica GmbH). The manufactured alloys are listed in Table 1. Quantitative chemical data from the manufactured alloys was obtained using OES spark analysis, and P content was measured by Glow Discharge Mass Spectroscopy (GDMS).

The alloy ingots of ~5 g were produced in an arc melter under a 200 mbar Ar atmosphere. The ingots were remelted three times, to ensure homogenization. The alloy charges of ~2.5–3 g were remelted in a quartz crucible (1 mm Ø orifice), in the melt-spinner and ejected (super heat $\Delta T = 125^\circ\text{C}$, $\Delta P = 100$ mbar) under reduced He (200 mbar) atmosphere onto a Cu wheel rotating with a wheel speed of 15 ms^{-1} , resulting in the production of ribbons ~3 mm wide and ~80 μm thick. To study the solidification behavior, ribbons of ~5 mg were investigated in the temperature range from 600°C to 400°C at a cooling rate of $10^\circ\text{C}/\text{min}$ in a power compensated DSC (Perkin-Elmer Diamond operated with Pyris7).

The ribbons were carefully ground and polished for optical examination (Zeiss Imager AXIO). SEM investigations were performed on an ESEM (FEI Quanta 200) equipped with EDX (Oxford Instruments INCA x-sight) system. Thin foil specimens for CTEM (Philips CM12, Conventional Transmission Electron Microscopy) were prepared on a Fischione twin-jet electropolisher. The samples were electropolished in an electrolyte containing 1/3 parts of HNO_3 and 2/3 parts of methanol at 0°C . Scheil simulation using ThermoCalc software with TTAL5 database was performed to predict the phases present in the alloys, their formation temperatures and their solidification range.

TABLE 1:

The manufactured binary and ternary alloys for the current investigation

Sr. No.	Alloy composition	Sr content (ppm)	P content (ppm)
1.	HP Al-5 wt. % Si	No add.	0.4
2.	MP Al-5 wt. % Si	No add.	<1
3.	MP Al-5 wt. % Si-Sr	50	
4.	MP Al-5 wt. % Si-Sr	100	
5.	MP Al-5 wt. % Si-Sr	1500	
6.	MP Al-5 wt. % Si-Sr	3000	

Note: HP stands for "High purity" and MP means "Medium purity" respectively. The purity level is defined on the basis of P content. (HP~0.4 ppm P, MP <1 ppm P)

3. Results

3.1 Microstructure of Melt-spun Ribbons

Figure 1 (a) is a bright field optical micrograph of an as-melt-spun ribbon from the HP Al- 5Si (wt. %) alloy. The microstructure consists of equiaxed Al grains (a few micrometers in size), silicon particles and eutectic droplets entrained within the Al matrix. The microstructure also reveals the presence of Al-Si eutectic distributed along the Al grain boundaries. Figure 1(b) shows the SEM backscattered image from the same alloy ribbons. The wide size distribution of the droplets can also be evident from the micrograph. The microstructure was not clear at such low magnifications, so, for a detail examination TEM investigations were necessary.

Figure 2(a) represents a bright field (BF) TEM image of one such eutectic droplet embedded within the Al matrix. As can be seen in Fig. 2(a), the droplet consisted of very fine (0.25–1 μm) silicon particles randomly dispersed between small equiaxed Al grains (Fig. 2(b)). There was a tendency for Si to be observed at the Al matrix interface.

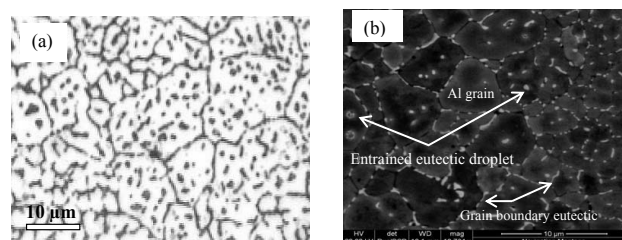


Fig. 1: (a) Bright field optical micrograph of HP Al-Si as melt-spun ribbon showing the distribution of eutectic at the grain boundary and within the matrix, (b) SEM backscattered image of the same alloy

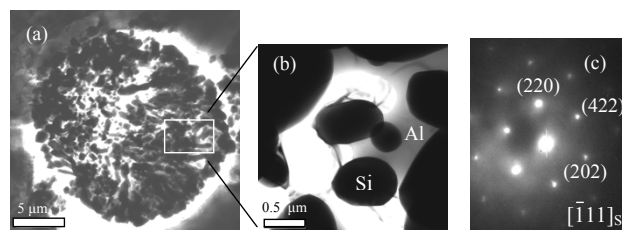


Fig. 2: (a) Bright field TEM image of eutectic droplet after DSC for MP Al-5 wt. % Si alloy, (b) within the droplet at higher magnification, and (c) corresponding diffraction pattern

Figure 2(c) shows the diffraction pattern taken from a silicon particle in the droplet tilted to its [111] zone axis. Figs. 3 (a) and (b) show twinned silicon particles, ~100–150 nm in size, within the Al matrix in as-melt-spun MP Al-5Si (wt. %) -50 ppm Sr alloy. The twinning of the silicon particles suggested that ΔT was significantly large for the formation of twins, although the resolution of the TEM was not sufficient to observe Sr at the re-entrant edges. ΔT is defined on the DSC trace (see Fig. 4(c)) which is the difference between the onset temperatures of grain boundary and droplet eutectic ($(T_E)_{G,B} - (T_E)_{D,E}$) i.e. $\sim 41^\circ\text{C}$. Twins were only observed when preferentially orientated and their apparent density appears low because only small areas were investigated.

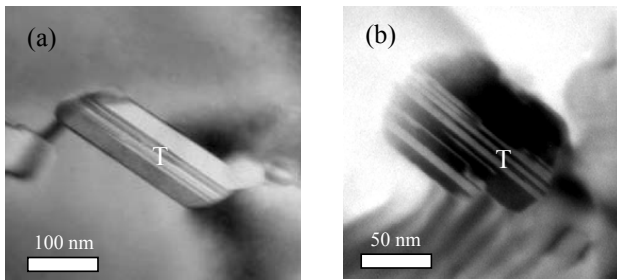


Fig. 3: (a) and (b) Twinned silicon particles within the Al matrix in as-melt-spun MP Al-5 wt. % Si-50 ppm Sr alloy

3.2 DSC Investigation

DSC investigations were performed to examine the effect of impurities on the droplet eutectic undercooling. Figures 4(a) and (b) show the DSC traces obtained from the melt-spun, medium and high purity alloys. Each thermogram revealed two distinct solidification exotherms (A & B) at a cooling rate of 10°C/min. The first sharp exotherm A corresponded to the solidification of grain boundary eutectic which in both cases occurred at an onset temperature of approximately $\sim 574 \pm 0.5^\circ\text{C}$, which is 3°C below the Al-Si equilibrium eutectic temperature documented in the literature¹⁵. The smaller exotherm B occurred at onset temperatures of $\sim 553 \pm 0.5^\circ\text{C}$ and $\sim 543 \pm 0.5^\circ\text{C}$ for the medium and

high purity alloys i.e. at undercoolings (ΔT) of 21°C and 31°C, respectively.

At least three runs for each sample were performed to check the reproducibility. It was found that all the DSC traces were reproducible within $\pm 0.5^\circ\text{C}$ at a cooling rate of 10°C/min, both for the medium and high purity Al-5Si (wt. %) alloys. Figures 4(c)-(f) show the DSC traces for the medium purity alloys with different levels of strontium (Sr) additions.

As it is evident from Fig. 4(c), a Sr addition of only 50 ppm to the medium purity alloy resulted in an increase in the eutectic droplet nucleation undercooling to 41°C. On increasing the amount of Sr further from 50 to 100 ppm or more, a third exothermic peak emerged i.e. exotherm C, in the DSC traces with an onset temperature of $565.5 \pm 0.5^\circ\text{C}$ (see Figures 4 (d) (e) and (f)). This peak represents the precipitation of a low temperature $\text{Al}_2\text{Si}_2\text{Sr}$ intermetallic phase just after (with respect to cooling) the solidification of grain boundary eutectic, exotherm A. Table 2 lists the measured entrained eutectic droplet undercooling ΔT with respect to the effect of Sr addition. Figure 5(a) shows the DSC solidification exotherm for the medium purity Al-5 wt. % Si binary alloy with the addition of $\sim 3\text{--}4$ ppm of phosphorus. Only the shoulder of the exotherm B can be observed on the DSC trace. Deconvolution of the

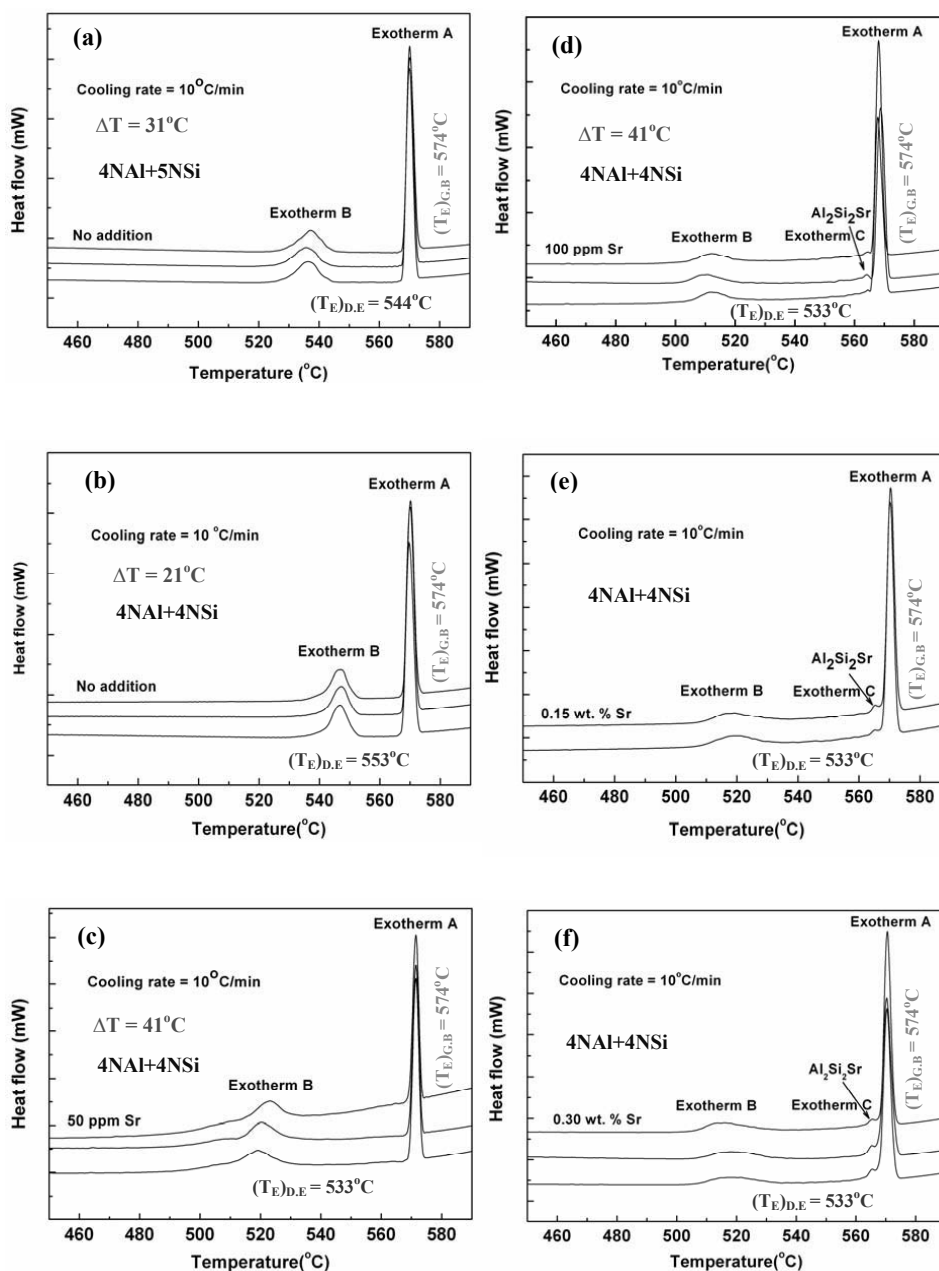


Fig. 4: (a) and (b) DSC solidification exotherms for HP and MP binary Al-Si alloys showing the difference of undercooling and (c)-(f) DSC traces for ternary Al-Si-Sr alloys with different addition levels of Sr at a cooling rate of 10°C/min

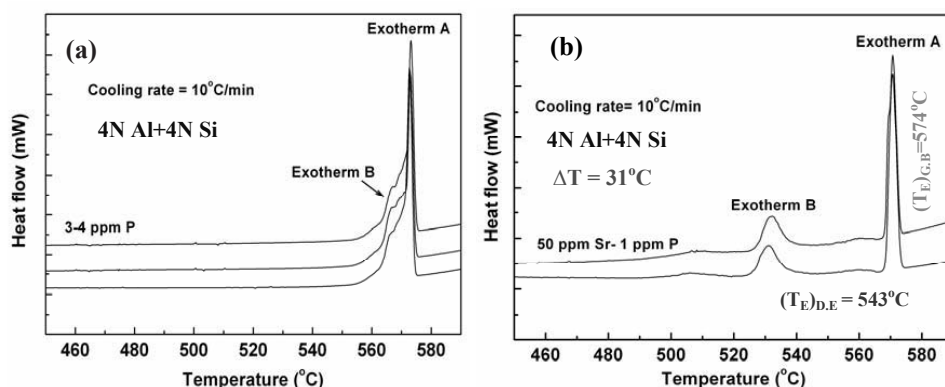


Fig. 5: (a) DSC traces for MP Al-5 wt. % Si-3-4 ppm P, and (b) for MP Al-5 wt. % Si- 50 ppm Sr-1 ppm P alloys at a cooling rate of 10°C/min

peak would be required in order to estimate the onset temperature. Figure 5(b) illustrates the DSC trace for the medium purity alloy with the additions of 50 ppm of Sr and 1 ppm of P only. The onset temperature for exotherm B was found to be $543 \pm 0.5^\circ\text{C}$, which is 10°C lower compared to the addition of 50 ppm Sr only, in the same alloy.

TABLE 2:

The amount of eutectic droplet (ΔT) measured at different Sr additions level

Alloy composition	Undercooling (ΔT) (oC)
HP Al-5 wt. % Si	31
MP Al-5 wt. % Si	21
MP Al-5 wt. % Si-50 ppm Sr	41
MP Al-5 wt. % Si-50 ppm Sr-1 ppm P	31

3.3 Scheil Simulation

The alloys liquidus and solidus temperatures, the expected phases and their approximate weight fraction were meas-

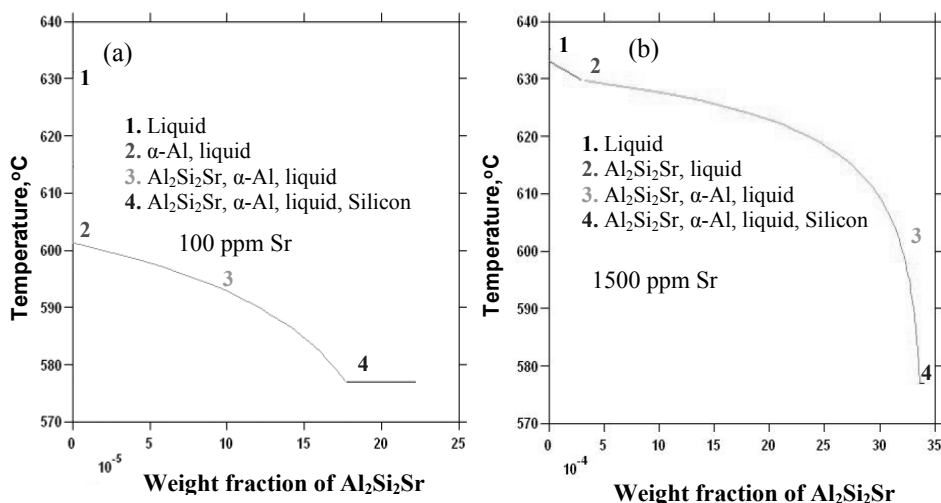


Fig. 6: Scheil simulation performed using TTAL5 database (a) weight fraction of $\text{Al}_2\text{Si}_2\text{Sr}$ in Al-5wt. %Si-100 ppm Sr, and (b) in Al-5wt. % Si-1500 ppm Sr alloy. The labelled number indicates the solidification range of the solid phase present

ured using the Scheil module from the TCCTM version of the ThermoCalc software in conjunction with its TTAL5 database. Figures 6(a) and (b) show the formation temperature and the solidification range of an $\text{Al}_2\text{Si}_2\text{Sr}$ intermetallic phase, for two different levels of Sr addition. The solidification range as well as weight fraction of $\text{Al}_2\text{Si}_2\text{Sr}$ phase were found to increase with increasing levels of strontium (Sr).

4. Discussion

4.1 Ribbon Microstructure and ΔT

The melt-spun Al-5wt. % Si binary alloys (both HP and MP), with no additions, solidified with two exothermic peaks. The sharp exotherm A expresses the solidification of grain boundary eutectic; whilst the smaller exotherm B represents the solidification of separate eutectic droplets within the Al matrix (see Figs. 4 (a) and (b)). The microstructure of the two phase eutectic droplet in the medium purity alloy, as shown in Fig. 2(a), indicates that there is a predominant shell of Si at the periphery of the eutectic droplet. The presence of the silicon at the interface between the droplet wall and Al matrix suggests that the silicon is nucleated by the surrounding Al matrix. These results are in good agreement with Ho et al. ⁶. They reported that traces of phosphorus i.e. 0.25–2 ppm are enough to form AlP. The P content in the alloys investigated here is >1 ppm (see Table 1). This quantity is sufficient to form AlP and hence nucleate the eutectic silicon at the interfaces, as proposed by Ho ⁶.

Since only CTEM was employed during this research work, no evidence of AlP was found at the interfaces because of the limited resolution of the microscope used. The random distribution of Si particles within the droplets suggests that the multiple nucleation of silicon particles¹⁶ occurs within the droplet.

Figure 4 (b) shows the DSC traces for the medium purity alloy. In the medium purity (MP) alloy only ~ 1 ppm of phosphorus is present. This suggests that the amount of phosphorus and other impurities exerts major influence on the droplet eutectic nucleation temperature. It can therefore be concluded that the amount of undercooling depends upon the purity of the matrix. These results are consistent with previous literature ^{5, 16}.

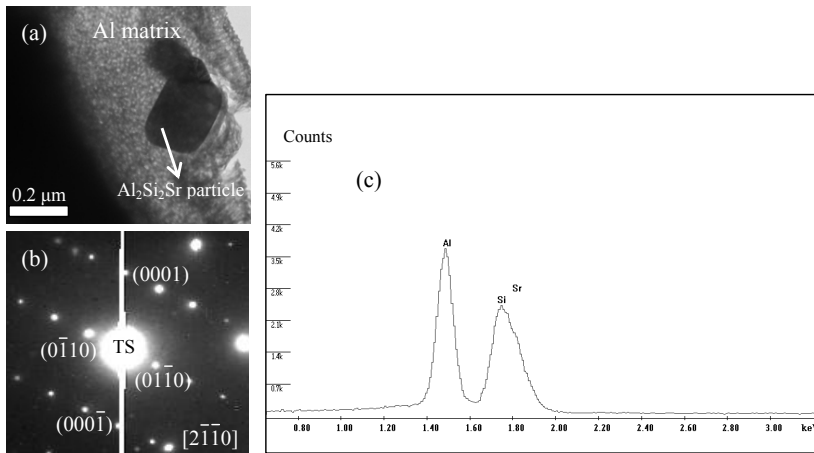


Fig. 7: (a) The BFTEM image of the melt spun MP Al-5wt. % Si-3000 ppm Sr ribbon showing an intermetallic $\text{Al}_2\text{Si}_2\text{Sr}$ phase, (b) SAD pattern and (c) corresponding EDX analysis

An addition of only 3–4 ppm of phosphorus in the medium purity Al-5Si (wt. %) binary alloy caused a significant shift of the smaller exotherm B towards exotherm A, this is evident from Fig. 5(a). Only the shoulder of this peak (exotherm B) can be observed. Published literature¹² suggests that the AIP phase is the major nucleation site for eutectic silicon because of the crystal structure and lattice parameter of AIP, both of which have an excellent lattice match with that of silicon. By increasing the P content in the binary alloy, higher quantities of the AIP compound are available in the melt, promoting the silicon nucleation in the droplet and reducing the amount of undercooling ΔT . These results support the theory that AIP is probably the most potent nucleation site for eutectic silicon.

The DSC trace for medium purity Al-5Si (wt. %)-50 ppm Sr-1 ppm P (see Fig. 5 (b)) shows an undercooling of 31 °C. The 10 °C decrease in the undercooling, compared with the addition of strontium only in the same alloy (see Fig. 4(c)), infer that even though Sr has a poisoning influence on the AIP compound, but due to an increase in the P content, some AIP is still available to nucleate the eutectic silicon at smaller undercooling (ΔT).

4.2 Effect of Sr

The addition of only 50 ppm of strontium in the medium purity alloy shifts the exotherm B towards higher undercoolings ΔT . This suggests that the addition of strontium depresses the droplet nucleation temperature. This may be because of the poisoning effect of strontium on the nucleation agent for silicon. The precipitation of Sr rich intermetallics i.e. $\text{Al}_2\text{Si}_2\text{Sr}$ at higher levels of strontium may act as a nucleation site for silicon in the absence of the AIP compound. The TEM investigation reveals the existence of a few nanometer sized (~200–300 nm) Sr intermetallic compounds i.e. $\text{Al}_2\text{Si}_2\text{Sr}$, within the Al matrix in the vicinity of the droplet in an Al-5Si (wt. %)-3000 ppm Sr alloy. This finding is supported by Scheil simulations which illustrate the precipitation of this compound before the eutectic reaction. Figs. 6 (a) and (b) show the outcome of the simulation for two different alloy compositions, having different levels of

strontium. The weight fraction and the solidification range of $\text{Al}_2\text{Si}_2\text{Sr}$ intermetallic both increase with higher levels of Sr.

Dahle et al.¹⁴ has suggested that if the Sr intermetallics nucleate on the AIP phase then insufficient number of nucleation sites are available for silicon and the nucleation of silicon should occur at larger undercooling. The current results suggest that after the consumption of the P with the formation of presumable amount of Sr_3P_2 compound the silicon nucleation subsequently occurs on $\text{Al}_2\text{Si}_2\text{Sr}$ compounds at larger undercooling. Figure 7(a) shows a bright field TEM image of an $\text{Al}_2\text{Si}_2\text{Sr}$ intermetallic particle, Fig. 7 (b) displaying the corresponding selected area diffraction pattern (SAD) taken by tilting to its zone axis [2-

1-1 0]. The indexing of the SAD pattern confirmed a hexagonal P-3mL ($a = 0.4187$ nm and $c = 0.7427$ nm) crystal structure. An EDX spectrum from the particle (shown in Fig. 7(c)) confirmed the elemental composition. The presence of these intermetallic particles in the Al matrix infers that this Sr rich intermetallic particle could nucleate eutectic silicon at larger undercooling when AIP is absent.

The presence of twinned silicon particles within the Al matrix indicates that impurity induced twinning (IIT) can play a major role in changing the morphology of the eutectic silicon, as proposed by Hellawell and co-workers^{6, 17}. However, no direct evidence of strontium at twin re-entrant edges was observed due to the limited resolution of the TEM used during this investigation. The present investigation reveals that the addition of Sr not only changes the silicon nucleation temperature but also enables the twinning. The modified silicon is then attributed to the effect of both of the above mentioned phenomena.

5. Conclusion

The entrained droplet technique has proved useful in the study of heterogeneous nucleation events within eutectic droplets. The additions of Sr in high purity Al-5Si (wt. %) alloys was found to depress the nucleation temperature of entrained eutectic droplets. With Sr additions of 100 ppm or higher, an $\text{Al}_2\text{Si}_2\text{Sr}$ intermetallic phase was formed. The precipitation of this low melting phase occurs before the nucleation of eutectic droplets can act as a nucleation site for silicon in the absence of AIP which is believed to be the most effective nucleation site for eutectic silicon. The poisoning of the AIP by strontium (formation of Sr_3P_2 compound) may force the eutectic silicon to nucleate at higher undercoolings ΔT on $\text{Al}_2\text{Si}_2\text{Sr}$ intermetallics.

Acknowledgements

Mr. Zarif would like to thank Prof. Peter Schumacher for providing the necessary experimental facilities at the Chair of Casting Research, University of Leoben, Austria. The au-

thors would also like to thank Prof. G. Dehm at the Erich Schmidt Institute, Leoben, for access to the TEM facilities and Dr. Rashkova for assistance with TEM imaging. In addition, Muhammad Zarif acknowledges the financial support from the Higher Education Commission (HEC) of Pakistan and appreciates the managerial work from OOAD.

References

- 1 Davis, J.R. et al., eds.: *Metals Handbook, Casting*, vol.15 (Metals Park, OH: Amercian Society for Metals, 1998), 751.
- 2 Hellawell, A: *The Growth and Structure of Eutectics with Silicon and Germanium*, (Great Britain: Pergamon press, 1970), 72.
- 3 Pacz, A: U.S Patent No. 1387900, 1921.
- 4 Crosley, P.B., and L.F. Mondolfo: *AFS Trans.*, 74 (1966), 53–64.
- 5 Ho, C.R., and B. Cantor: *Acta Metall. Mater.*, 43 (8) (1995), 3231–3246.
- 6 Shu-Zu, Lu, and A. Hellawell: *Met. Trans. A*, 18A (1987), 1721–1733.
- 7 Wang, C.C., and C.S. Smith: *Transactions AIME*, 188 (1950), 136–138.
- 8 O'Reilly, K. A. Q., and B. Cantor: *Acta Metal. Mater.*, 43 (2) (1995), 405–417.
- 9 Moore, K. I., Zhang D. L., and B. Cantor: *Acta Metal. Mater.*, 38 (7) (1990), 1327–1342.
- 10 Kim, W. T., and B. Cantor: *Acta Metall. Mater.*, 40 (9) (1992), 3339–3347.
- 11 Ho, C.R., and B. Cantor: *J. Mater. Sci.*, 20 (1995), 1912–1920.
- 12 Nogita, K., S.D. McDonald, K. Tsujimoto, K. Yasuda, and A.K. Dahle: *J. Electron Microscopy*, 53 (2004), 361–369.
- 13 Bäckerud, L., G. Chai, and J. Tamminen: *Solidification Characteristics of Aluminium Alloys*, Vol. 2 Foundry Alloys, AFS Company U.S.A, 1990, 37.
- 14 Cho, Y.H., H.C. Lee, K. H. Oh, and A.K. Dahle: *Metall. Mater. Trans. A*, 39A (2008), 2435–2448.
- 15 Murray, J.L., and A.J. McAlister: *Bulletin of Alloy Phase Diagrams*, 5 (1) (1984), 74–84.
- 16 Zhang, D.L., and B. Cantor: *Metall. Trans. A*, 24A (1993), 1195–1204.
- 17 Hanna, M.D., Shu-Zu Lu, and A. Hellawell: *Met. Trans. A*, 15A (1984), 459–469.